

Cavity enhanced transport of excitons

Johannes Schachenmayer,¹ Claudiu Genes,² Edoardo Tignone,³ and Guido Pupillo³

¹*JILA, NIST, Department of Physics, University of Colorado, 440 UCB, Boulder, CO 80309, USA*

²*Institut für Theoretische Physik, Universität Innsbruck, Technikerstrasse 25, A-6020 Innsbruck, Austria*

³*IPCMS (UMR 7504) and ISIS (UMR 7006), Université de Strasbourg and CNRS, Strasbourg, France*
(Dated: July 19, 2022)

We show that exciton-type transport in certain materials can be dramatically modified by their inclusion in an optical cavity: the modification of the electromagnetic vacuum mode structure introduced by the cavity leads to transport via delocalized polariton modes rather than through tunneling processes in the material itself. This can help overcome exponential suppression of transmission properties as a function of the system size in the case of disorder and other imperfections. We exemplify massive improvement of transmission for excitonic wave-packets through a cavity, as well as enhancement of steady-state exciton currents under incoherent pumping. These results have direct implications for experiments with disordered organic semi-conductors. We propose that the basic phenomena can be observed in quantum simulators made of Rydberg atoms, cold molecules in optical lattices, as well as in experiments with trapped ions.

Understanding the transport properties of quanta and correlations and how to make this transport efficient over large distances are questions of fundamental importance in a variety of fields, ranging from experiments with cold atoms and ions [1–4], to quantum information theory [5–7], to (organic) semiconductor and solar cell physics [8–10]. In most realistic situations, transport efficiency is known to be strongly inhibited by disorder. For example, Anderson-type localization of single-particle eigenstates [11] in disordered media implies an *exponential* suppression of exciton transmission, i.e. over a distance of N sites it decays as $T \propto \exp(-N)$. This is the case, e.g., with energy transport in organic semiconductors based on Frenkel excitons (i.e. electron-hole pairs) [8], where disorder occurs, e.g., in the spatial distribution, dipole orientations and internal energies of the molecules. Inspired by first breakthrough experiments on charge transport in these molecular semiconductors in the strong-coupling regime [12], in this work we show how this exponential suppression can be essentially overcome by coupling the excitons to the structured vacuum field of a Fabry-Perot cavity placed transverse to the direction of exciton propagation. In one dimension, this trades the exponential suppression for a decay which is at most *algebraic*, $T \propto N^{-2}$, a massive enhancement that should be observable for realistic exciton-cavity couplings, system sizes, disorder strengths and even at room temperature [12–22]. In principle, this effect may open the way towards utilizing molecular materials as inexpensive and flexible alternatives to traditional silicon-based semiconductors [8, 23–29].

Here, we provide a theoretical understanding of enhanced exciton transport for a model of two-level systems embedded in a cavity in the limit of strong collective light-exciton coupling, which closely resembles the configuration of Refs. [12, 17, 18]. We note that in these systems, strong collective coupling has been already demonstrated, and even used, e.g., to modify intrinsic material

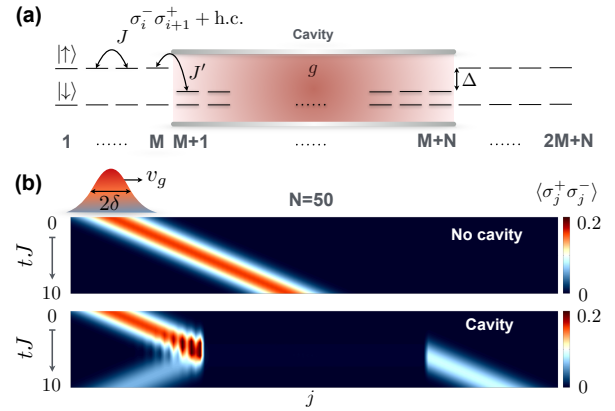


FIG. 1. *Exciton transmission model.* Scheme of a chain of coupled two-level systems (tunneling rate J) in which an exciton wave-packet (width δ) propagates from the left with group velocity v_g into a cavity that is coupled to N spins (cavity-spin coupling g). Under the right conditions, a large portion of the wave-packet can be almost instantaneously transmitted to the right side in a timescale $t \ll N/v_g$, as shown in the example in panel (b) ($N = 50, M = 20, v_g = 2J, \delta = 3, \Delta = 69J, J' = 10J, g = 10J$, see text).

properties such as the work function [30]. Our model also applies to artificial media such as cavity-embedded Rydberg lattice gases [31, 32], polar molecules in optical lattices [33, 34], or ions in linear Paul traps [35, 36]. In these systems, large couplings [37] and reduced decoherence from spontaneous emission may allow for demonstrating essentially instantaneous coherent transport of excitonic wave-packets over large distances with close-to-unit efficiency, $T \propto 1$.

The model we consider consists of a chain of N two-level systems or “spins” with local states $|\uparrow\rangle_i$ and $|\downarrow\rangle_i$ that are embedded in a cavity. The coupling to the cavity mode is governed by the Tavis-Cummings Hamiltonian $H_{\text{cav}} = g \sum_i (\sigma_i^+ a + \sigma_i^- a^\dagger)$, with g the coupling strength, a (a^\dagger) the destruction (creation) operator for

the cavity photon, and σ_i^\pm the Pauli spin raising/lowering operators for the spin at site i . The excitations (i.e. the states $|\uparrow\rangle_i$) have an energy ω_i ($\hbar \equiv 1$) and can tunnel between neighboring sites, as described by the Hamiltonian $H_0 = \sum_i [\omega_i \sigma_i^+ \sigma_i^- - J_i (\sigma_i^+ \sigma_{i+1}^- + \sigma_i^- \sigma_{i+1}^+)]$. The tunneling rates J_i can be site-dependent, and we define $J_i = J + \delta J_i$, where δJ_i denotes random disorder drawn from a normal distribution.

The general dynamics of our system is governed by the master equation $\dot{\rho} = -i[H, \rho] - \sum_\alpha \mathcal{L}_\alpha(\rho)$, with ρ the density matrix and $H = H_0 + H_{\text{cav}}$. The terms $\mathcal{L}_\alpha(\rho) \equiv -\{L_\alpha^\dagger L_\alpha, \rho\} + 2L_\alpha \rho L_\alpha^\dagger$ incorporate all dissipative processes via ordinary Lindblad operators L_α . We consider for example cavity decay ($L_\kappa \equiv \kappa a/2$) as well as spontaneous emissions of each spin ($L_{\text{sp.em.},i} \equiv \gamma_{\text{sp.em.}} \sigma_i^-/2$) or dephasing ($L_{\text{deph.},i} \equiv \gamma_{\text{deph.}} \sigma_i^+ \sigma_i^-/2$), deriving e.g. from radiative decay and fluctuations in level-spacing (vibrations), respectively. In the homogeneous situation with $\omega_i = \omega_0$ and $J_i = 0$, H_{cav} is responsible for the formation of dressed modes of the cavity photons and of the collective Dicke states $\sigma_0^\pm \equiv \sum_j \sigma_j^\pm / \sqrt{N}$, named as upper and lower polaritons for $u^\dagger \equiv (a^\dagger + \sigma_0^+)/\sqrt{2}$ and $d^\dagger \equiv (a^\dagger - \sigma_0^+)/\sqrt{2}$, respectively, with energy $\Omega_{u,d} = \omega_0 \pm g\sqrt{N}$. In this work we study two possible scenarios to observe enhancement of exciton transport by exploiting these polariton states: (i) a wave-packet scattering experiment, and (ii) steady state exciton currents under incoherent pumping. The latter may be of interest for, e.g., artificial media and molecular semiconductors, respectively.

Case (i) is sketched in Fig. 1(a): In addition to the N spins in the cavity, M spins are added to the left and right of the cavity ($\mathcal{N} = 2M + N$), with Hamiltonian H_0 . We consider a homogeneous level-spacing inside and outside of the cavity, with $\omega_i = \omega_0$ for $i = M + 1, \dots, M + N$ and $\omega_i = \omega$ otherwise, and define the relative detuning $\Delta = \omega - \omega_0$. We further denote $J_i = J'$ for $i = M + 1$ and $i = M + N$, i.e., at the entrance and exit of the cavity, to allow for impedance effects (see below). At time $t = 0$, a Gaussian-shaped wave-packet of excitons, $|\psi(t=0)\rangle \propto \sum_{j=1}^{\mathcal{N}} e^{-iq_0 j} e^{-(j-j_0)^2/(4\delta^2)} |j\rangle$, with width δ (standard deviation) and initial quasi-momentum q_0 is injected on the left. Here, $|j\rangle \equiv |\uparrow\rangle_j \otimes_{i \neq j} |\downarrow\rangle_i$ denotes the state of a single excitation at site j . The initial displacement from the cavity is $\delta_x = M - j_0$. As an example, we choose $\delta_x = 20$, $\delta = 5$ and $q_0 = \pi/2$ [corresponding group velocity $v_g = 2J \sin(q_0) = 2J$]. We are interested in the wave-packet fraction that for properly tuned parameters can be transferred nearly instantaneously to the right side of the cavity upon scattering [cf. Fig. 1(b)].

Case (ii), in contrast, concerns a system with sites $i = 1, \dots, N$ embedded in the cavity. Excitations are incoherently pumped to site $i = 1$ from the left and are removed from site $i = N$. This can be achieved via dissipative terms with $L_P \equiv \gamma_P \sigma_1^+/2$ and $L_{\text{out}} \equiv \gamma_{\text{out}} \sigma_N^-/2$, respectively. Under these conditions, we calculate the

output current of excitons, $I_{\text{out}} = \text{tr}[n_e \mathcal{L}_{\text{out}}(\rho)]$ (with $n_e = \sigma_N^+ \sigma_N^-$) in the steady-state. Similar to the case [38], this current arises naturally from the continuity equation $d\langle n_e \rangle/dt = 0 = \text{tr}[n_e \mathcal{L}_P(\rho)] + \text{tr}[n_e \mathcal{L}_{\text{out}}(\rho)] + \text{tr}[n_e \mathcal{L}_{\text{sp.em.}}(\rho)] + \text{tr}[n_e \mathcal{L}_{\text{deph.}}(\rho)] - i\text{tr}[n_e [H, \rho]]$. In the second part of this paper we show how I_{out} can be dramatically enhanced in the presence of the cavity.

Wave-packet scattering – In case (i), we first simplify the dynamics by neglecting all dissipative terms and disorder (a very good approximation for e.g. a Rydberg lattice gas [39]). Under these conditions, for $g = 0$ the wave-packet ($v_g = 2J$) reaches the right side of the cavity on a long timescale $t_l J = \delta_x + 2\delta + N/2$. This is essentially the time required to hop over N sites plus the time needed to enter and exit the cavity, and corresponds to light-cone-type propagation. Here we propose to use the polariton mode to tunnel N sites almost instantaneously.

The time-scale for a single excitation to couple in and out of the collective polariton mode is proportional to \sqrt{N}/g , and can be exceedingly small for g large enough. Then, transmission to the right side beyond the free-evolution light-cone is possible on an *ultra-short* scale $t_s J = \delta_x + 2\delta \ll t_l J$, which is dominated by the entrance time in the cavity. The dynamics can then be described via elastic scattering through the cavity, with a quasi-momentum dependent transmission function $T_q = |t_q|^2$, and t_q the coefficient appearing in the associated Lippmann-Schwinger scattering equation [40].

The time-independent function T_q completely determines the conduction properties of the material [41–44], and can be computed exactly for our model. The coefficient has the general form $t_q = -2i\beta/[1 + 2i\beta]$, with $\beta = [2NJ \sin(q)]^{-1} \sum_n |J'|^2 / [\omega - 2J \cos(q) - \tilde{\Omega}_n]$. Here, $\tilde{\Omega}_n$ is the n th eigenvalue of the reduced Hamiltonian for the cavity-coupled central N sites of the chain [39]. The resulting T_q in general presents three regions of ballistic transmission (i.e., $T_q = 1$). These correspond to (a) ordinary exciton hopping for $\Delta \sim 0$, with an approximate width $4J$, as well as (b) two peaks for $\Delta \sim \Omega_{u,d} - J$. The latter correspond to polariton-mediated transmission, and have an approximate Lorentzian shape with a N -dependent full width at half maximum (FWHM) $w = J'^2/(N|v_g|)$. For large enough strength of the collective exciton-cavity coupling $g\sqrt{N} > \max[w, 4J, \kappa]$ all peaks are well separated, which defines the *collective strong coupling* regime. In the following we focus on this regime, where in the vicinity of the polariton peaks T_q is found to simplify to

$$T_q = \{1 + N^2 J^2 \sin^2(q) [\omega + J(1 - 2\cos(q)) - \Omega_{u,d}]^2 / J'^4\}^{-1}. \quad (1)$$

The full time-dependent scattering dynamics for the initial wave-packet, $|\psi(t=0)\rangle$ can be investigated via a numerical exact diagonalization technique. We thus de-

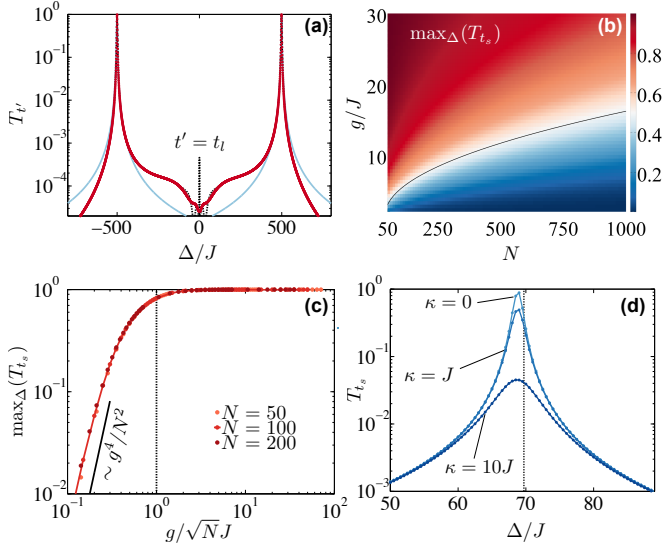


FIG. 2. *Ultra-fast transmission* of a wave-packet with $\delta = 5$, $\delta_x = 20$, and $q_0 = \pi/2$ ($v_g = 2J$). We choose $J' = 4\tilde{J}_N$ (see text). (a) The long time and ultra-short transmission T_{t_l} and T_{t_s} , respectively, as function of Δ . The cavity embeds $N = 100$ sites and $g = 50$ (deep strong collective coupling regime). Clearly, one can identify two peaks of T_{t_s} and T_{t_l} at the two polariton energies. The numerical calculation (red line) agrees with expected analytical result (blue line). T_{t_l} also contains a small $\Delta \sim 0$ peak, corresponding to free evolution. (b) $\max_{\Delta}(T_{t_s})$ as function of g and N (Δ is tuned to obtain maximum T_{t_s} for $\Delta \sim \Omega_u$). To keep the ultra-fast transmission fixed, $g \propto \sqrt{N}$ (solid line) is required. (c) Crossover into the regime of large ultra-fast transmission around $g \sim \sqrt{N}J$ (dashed line). $\max_{\Delta}(T_{t_s})$ for $N = 50, 100, 200$ is shown as function of g/\sqrt{N} (on top of each other). For small g , $T_{t_s} \sim g^4/N^2$ (solid line). (d) Shrinkage and broadening of transmission peaks for finite cavity decay κ ($N = M = 50$, $g = 10J$)

fine the following time-dependent transmission

$$T_{t'} = \sum_{j > M+N} \langle \sigma_j^+ \sigma_j^- \rangle_{t'}. \quad (2)$$

This observable measures the total number of excitations that reach the right side of the system at a given time t' .

Our goal is to realize large ultra-fast transmission via the polariton peaks with $T_{t'} \sim 1$ and $t' = t_s$. Thus two conditions have to be met: (i) The detuning Δ has to match the energy of either of the polariton peaks; and (ii) the wave-packet has to be sufficiently sharp in quasi-momentum space to fit into the energy window w , implying a real-space width on the order of the cavity length. While this can be generally difficult to realize, we find that condition (ii) can be satisfied by a choice $J' \propto \tilde{J}_N \equiv (2 \ln 2)^{1/4} \sqrt{N/2\delta}J$ (ensuring that w remains independent of N), similar to an impedance effect.

In Fig. 2(a) we compare $T_{t'}$ for different Δ , for $t' = t_s$ (red continuous line) and $t' = t_l$ (black dashed line). We

choose a cavity with $N = 100$ sites, a large $g = 50J$, and set $J' = 4\tilde{J}_N$. As expected, here the figure shows the existence of two distinct polariton peaks, allowing for ballistic transmission on the ultra-fast scale t_s . The position and width of the peaks are in agreement with the analytical time-independent predictions of Eq. (1). The peak at $\Delta \sim 0$ instead reflects regular exciton hopping on a time-scale $t_l \gg t_s$. Note that here $T_{t_l} < 1$ due to backscattering at the cavity entrance where $J' > J$.

When decreasing the coupling strength g , the exciton dynamics through the cavity slows down considerably [39]. The scattering becomes generally inelastic within t_s : part of the wave-packet energy remains in the cavity and $T_{t_s} < 1$. However, we find that even for moderate couplings, a large fraction of the exciton wave-packet can be still transmitted within t_s . This is shown in Fig. 2(b), which is a contour plot of $\max_{\Delta}(T_{t_s})$ (i.e. the best transmission achieved for Δ chosen in the vicinity of the upper polariton energy) as a function of g and N : For increasing N , T_{t_s} remains large and constant for a choice $g \sim \sqrt{N}J$ [solid black line]. In addition, Fig. 2(c) shows that T_{t_s} vs $g/\sqrt{N}J$ displays a universal behavior for different system sizes N . Here, T_{t_s} reaches large values $\sim 80\%$ for $g = \sqrt{N}J$ improving to 100% when increasing $g/\sqrt{N}J$. This is expected since for $g > \sqrt{N}J$, we enter the elastic scattering regime, in which the time-scale for coupling in and out of the polariton mode becomes negligible. We thus note that in this regime an ultra-fast transmission with $T_{t_s} \sim 1$ over arbitrarily large distances N becomes possible, if a coupling strength $g \gtrsim \sqrt{N}J$ can be engineered. Interestingly, the figure shows that even for $g \ll \sqrt{N}J$ a significant part of the wave-packet is transmitted within t_s . In this regime, which corresponds to inelastic scattering in the collective strong coupling regime, we find the general scalings $T_{t_s} \sim g^4$ and $T_{t_s} \sim 1/N^2$. Thus, cavity-mediated transmission decreases only *algebraically* with N , which can be important, e.g., when competing against exponential suppression due to disorder. We come back to this point below.

In the case of a lossy cavity ($\kappa \neq 0$), the effect of dissipation is in general to decrease T_{t_s} with increasing κ , due to loss of exciton population, while the FWHM increases accordingly. In Fig. 2(d) we show that ultra-fast transmission of a large wave-packet fraction is however still possible for $\kappa \sim J$ (as, e.g., in a polar molecule setup, see [39]). There, the dynamics after an adiabatic elimination of the cavity mode can be effectively described by an all-to-all hopping Hamiltonian $H_{\text{eff}} \approx \frac{2g^2}{\kappa} \sum_{i,j} \sigma_i^- \sigma_j^+$. Similar to H_{cav} above, we find that also H_{eff} can give rise to ultra-fast transmission. We propose that such a situation could for example be observed in experiments with trapped ions, where these type of very long-ranged interactions arise naturally even in the absence of a cavity [39].

In realistic organic semi-conductors, disorder is key both in the spatial distribution and dipole orientation

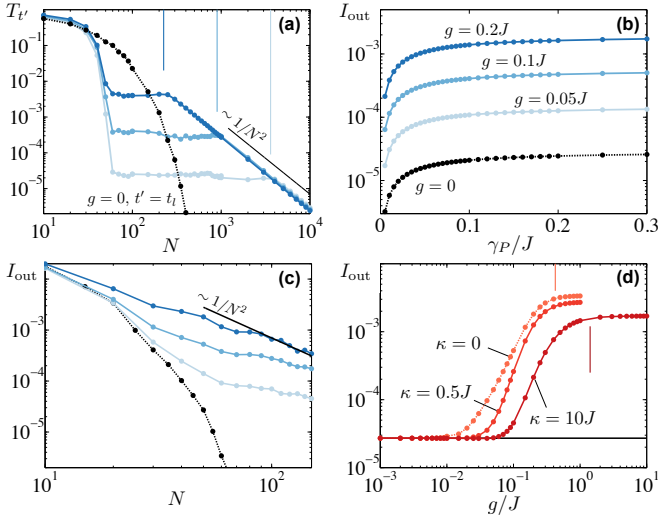


FIG. 3. *Organic semiconductor situation*— Weakly coupled cavity results are indicated by blue lines/points [from light to dark] for $g = 0.05J, 0.1J, 0.2J$, respectively, $g = 0$ by a black dashed line with points. (a) T_{ts} and T_{tl} for wave-packet scattering identical to the one in Fig. 2. $\Delta = g\sqrt{N} - J$. We average over 200 Gaussian disorder realizations in J_i ($\delta_J = 0.2J$). For $g = 0$ we plot T_{tl} , for $g > 0$ T_{ts} as function of N . T_{tl} decreases exponentially with system size, whereas the cavity-assisted T_{ts} becomes system independent in the weak coupling regime and decays as $1/N^2$ [black solid line] in the collective strong coupling regime. The transition to this regime is indicated by the vertical lines, which mark $g\sqrt{N} = 3J$, respectively. (b) Steady state exciton current I_{out} for $N = 50$ cavity embedded sites with disorder, spontaneous emissions, and dephasing. Excitations are pumped into the system on one cavity entrance with rate γ_P and removed on the other with $\gamma_{out} = 2J$. Small g already leads to a massive enhancement. (c) As function of N , because of all dissipative terms and disorder I_{out} decays exponentially ($\gamma_P = 0.5J$), while for $g > 0$ it decays much slower with N . In the collective strong coupling regime, $I_{out} \sim 1/N^2$ [black solid line]. (d) I_{out} as function of g , showing the crossover to the collective strong coupling regime and its dependance on a finite cavity decay κ ($N = 50$, $\gamma_P = 0.5J$). Vertical lines indicate $g\sqrt{N} = 3J$ and $g\sqrt{N} = 10J$, respectively. For panels (b-d): $\gamma_{sp.em.} = 0.04J$, $\gamma_{deph.} = 0.9J$, and $\delta_J = 0.2J$, single noise realization.

of molecules, implying site-dependent J_i in H_0 . In addition, typical cavity couplings are much weaker ($g \sim 0.1J$) as in the artificial material above (see [39]). Figure 3(a) shows $T_{t'}$ as function of N for the same setup of Fig. 2, with $\delta_J = 0.2$ but for fixed $\Delta = g\sqrt{N} - J$. Without cavity ($g = 0$) T_{tl} is exponentially suppressed, leading essentially to zero transmission for large N ($T_{ts} < 10^{-6}$ for $N \gtrsim 400$ sites), as expected from Anderson-type localization in one-dimension [11]. However, the localized eigenstates of the system can be modified by the cavity [45–47]. Adding realistically weak cavity couplings ($g = 0.05J, 0.1J, 0.2J$) already lifts the transport suppression and allows for a small but finite transmission even for systems with $N = 10000$ sites. Consistent with

the discussion above, in the collective strong coupling regime [right of vertical lines] we find an universal algebraic behavior $T_{t'} \sim 1/N^2$. Interestingly, also in the weak coupling regime [left of vertical lines], i.e. when the two polariton peaks cannot be resolved, we find a small but essentially constant transmission which is orders of magnitudes larger than T_{tl} in the cavity-free case.

Incoherent pumping setup – We now consider the case (ii) above, resembling the experiment of [12], where we analyze steady-state currents I_{out} that develop under incoherent pumping of excitations ($\gamma_P, \gamma_{out} > 0$). In addition to disorder, spontaneous emission and dephasing are now included with $\gamma_{sp.em.} = 0.04J$ and $\gamma_{deph.} = 0.9J$, respectively. The pump rate γ_P plays the role of a “voltage” for the exciton currents, and we can plot “I-V curves” for the exciton current, Fig. 3(b). The figure shows that even small cavity couplings g can increase I_{out} by orders of magnitude compared to the cavity-free case ($g = 0$). This finding is in stark contrast with previous works with exciton-polariton in multi-mode cavities [48] and constitutes one of the key results of this work.

Consistent with the wave-packet dynamics above, Fig. 3(c) shows that, for $g = 0$, I_{out} decreases exponentially with N , due to the various dissipative terms and the disorder. However, again, adding a small $g = 0.05, 0.1, 0.2$, changes the currents dramatically: for $N = 150$ and $g = 0.2$ the collective strong coupling regime is barely reached $g\sqrt{N} \sim 2.5J$; nevertheless, remarkably, we find that I_{out} , just as T_{ts} above, already displays an algebraic large- N decrease proportional to $1/N^2$. The fact that the cavity enhancement of I_{out} is indeed induced by a collective coupling to the cavity mode is further demonstrated in Fig. 3(d), where I_{out} is shown vs g , for a few values of κ . There, we find a sudden increase of I_{out} when g exceeds a particular value, indicated by the vertical lines. By inspection, we find that this indeed corresponds to the point where $g\sqrt{N}$ exceeds all other energy scales. Consistently, this point is shifted to larger values of g for large $\kappa = 10$, see Fig. 3(d).

Conclusion & Outlook – In this work, we have shown that both incoherent and coherent exciton transport in a spin chain can be dramatically enhanced by collective coupling to the structured vacuum field of a Fabry-Perot cavity. These results may be relevant for disordered organic semiconductors at room-temperature, where conduction may be ameliorated by orders of magnitude, as well as for artificial media made of Rydberg atoms, polar molecules or cold ions at sub-mK temperatures. It is an exciting prospect to investigate whether strong coupling can induce the propagation of both classical and quantum correlations [49, 50] at ultrafast timescale in the case of interacting excitations [51].

We note that results for transport in disordered organic semiconductors related to those reported here have been independently obtained by J. Feist and F. J. Garcia-Vidal [52].

Acknowledgements— We thank T. W. Ebbesen, F. J. Garcia Vidal, J. Feist, L. M. Moreno and H. Ritsch for fruitful discussion. J.S. acknowledges hospitality from the Institute for Theoretical Physics at the University of Innsbruck and the University of Strasbourg. This work was supported by the ERC-St Grant ColdSIM (No. 307688), EOARD, and UoS via Labex NIE and IdEX, the JQI, the NSF PFC at the JQI, Initial Training Network COHERENCE, as well as the Austrian Science Fund (FWF) via project P24968-N27 (CG). Computations utilized the HPC UoS, and the Janus supercomputer, supported by NSF, NCAR and CU Boulder.

-
- [1] P. Jurcevic, B. P. Lanyon, P. Hauke, C. Hempel, P. Zoller, R. Blatt, and C. F. Roos, *Nature* **511**, 202 (2014).
 - [2] P. Richerme, Z.-X. Gong, A. Lee, C. Senko, J. Smith, M. Foss-Feig, S. Michalakis, A. V. Gorshkov, and C. Monroe, *Nature* **511**, 198 (2014).
 - [3] M. Cheneau, P. Barmettler, D. Poletti, M. Endres, P. Schauß, T. Fukuhara, C. Gross, I. Bloch, C. Kollath, and S. Kuhr, *Nature* **481**, 484 (2012).
 - [4] G. Günter, H. Schempp, M. Robert-de Saint-Vincent, V. Gavryusev, S. Helmrich, C. S. Hofmann, S. Whitlock, and M. Weidemüller, *Science* **342**, 954 (2013).
 - [5] S. Bose, *Contemporary Physics* **48**, 13 (2007), arXiv:0802.1224.
 - [6] E. H. Lieb and D. W. Robinson, *Communications in Mathematical Physics* **28**, 251 (1972).
 - [7] B. Nachtergaele, Y. Ogata, and R. Sims, *Journal of Statistical Physics* **124**, 1 (2006).
 - [8] S. R. Forrest, *Nature* **428**, 911 (2004).
 - [9] G. D. Scholes and G. Rumbles, *Nature Materials* **5**, 683 (2006).
 - [10] S. M. Menke, W. A. Luhman, and R. J. Holmes, *Nature Materials* **12**, 152 (2013).
 - [11] P. W. Anderson, *Physical Review* **109**, 1492 (1958).
 - [12] E. Orgiu, J. George, J. A. Hutchison, E. Devaux, J.-F. Dayen, B. Doudin, F. Stellacci, C. Genet, P. Samori, and T. W. Ebbesen, arXiv:1409.1900 (2014).
 - [13] D. G. Lidzey, D. D. C. Bradley, M. S. Skolnick, T. Virgili, S. Walker, and D. M. Whittaker, *Nature* **395**, 53 (1998).
 - [14] D. G. Lidzey, D. D. C. Bradley, T. Virgili, A. Armitage, M. S. Skolnick, and S. Walker, *Physical Review Letters* **82**, 3316 (1999).
 - [15] R. J. Holmes and S. R. Forrest, *Physical Review Letters* **93**, 186404 (2004).
 - [16] D. M. Coles, P. Michetti, C. Clark, W. C. Tsoi, A. M. Adawi, J.-S. Kim, and D. G. Lidzey, *Advanced Functional Materials* **21**, 3691 (2011).
 - [17] T. Schwartz, J. A. Hutchison, C. Genet, and T. W. Ebbesen, *Physical Review Letters* **106**, 196405 (2011).
 - [18] S. Kéna-Cohen, S. A. Maier, and D. D. C. Bradley, *Advanced Optical Materials* **1**, 827 (2013).
 - [19] J. D. Plumbhof, T. Stöferle, L. Mai, U. Scherf, and R. F. Mahrt, *Nature Materials* **13**, 247 (2014).
 - [20] R. Balili, V. Hartwell, D. Snoke, L. Pfeiffer, and K. West, *Science* **316**, 1007 (2007).
 - [21] E. Wertz, A. Amo, D. D. Solnyshkov, L. Ferrier, T. C. H. Liew, D. Sanvitto, P. Senellart, I. Sagnes, A. Lemaitre, A. V. Kavokin, et al., *Physical Review Letters* **109**, 216404 (2012).
 - [22] M. Alloing, M. Beian, M. Lewenstein, D. Fuster, Y. González, L. González, R. Combescot, M. Combescot, and F. Dubin, *EPL (Europhysics Letters)* **107**, 10012 (2014).
 - [23] H. Shirakawa, E. J. Louis, A. G. MacDiarmid, C. K. Chiang, and A. J. Heeger, *Journal of the Chemical Society, Chemical Communications* pp. 578–580 (1977).
 - [24] C. W. Tang and S. A. VanSlyke, *Applied Physics Letters* **51**, 913 (1987).
 - [25] J. H. Burroughes, D. D. C. Bradley, A. R. Brown, R. N. Marks, K. Mackay, R. H. Friend, P. L. Burns, and A. B. Holmes, *Nature* **347**, 539 (1990).
 - [26] C. Kim, P. E. Burrows, and S. R. Forrest, *Science* **288**, 831 (2000).
 - [27] A. Kahn, N. Koch, and W. Gao, *Journal of Polymer Science Part B: Polymer Physics* **41**, 2529 (2003).
 - [28] H. Sirringhaus, M. Bird, and N. Zhao, *Advanced Materials* **22**, 3893 (2010).
 - [29] A. C. Arias, J. D. MacKenzie, I. McCulloch, J. Rivnay, and A. Salleo, *Chemical Reviews* **110**, 3 (2010).
 - [30] J. A. Hutchison, A. Liscio, T. Schwartz, A. Canaguier-Durand, C. Genet, V. Palermo, P. Samori, and T. W. Ebbesen, *Advanced Materials* **25**, 2481 (2013).
 - [31] R. Löw, H. Weimer, J. Nipper, J. B. Balewski, B. Butscher, H. P. Büchler, and T. Pfau, *Journal of Physics B: Atomic, Molecular and Optical Physics* **45**, 113001 (2012).
 - [32] S. Bettelli, D. Maxwell, T. Fernholz, C. S. Adams, I. Lesanovsky, and C. Ates, *Physical Review A* **88**, 043436 (2013).
 - [33] B. Yan, S. A. Moses, B. Gadway, J. P. Covey, K. R. A. Hazzard, A. M. Rey, D. S. Jin, and J. Ye, *Nature* **501**, 521 (2013).
 - [34] K. R. A. Hazzard, B. Gadway, M. Foss-Feig, B. Yan, S. A. Moses, J. P. Covey, N. Y. Yao, M. D. Lukin, J. Ye, D. S. Jin, et al., arXiv:1402.2354 (2014).
 - [35] D. Porras and J. I. Cirac, *Physical Review Letters* **92**, 207901 (2004).
 - [36] A. Friedenauer, H. Schmitz, J. T. Glueckert, D. Porras, and T. Schaetz, *Nature Physics* **4**, 757 (2008).
 - [37] J. M. Raimond, M. Brune, and S. Haroche, *Reviews of Modern Physics* **73**, 565 (2001).
 - [38] D. Manzano, M. Tiersch, A. Asadian, and H. J. Briegel, *Phys. Rev. E* **86**, 061118 (2012).
 - [39] Supplemental Material (below).
 - [40] D. A. Ryndyk, R. Gutierrez, B. Song, and G. Cuniberti, arXiv:0805.0628 (2008).
 - [41] R. Landauer, *IBM Journal of Research and Development* **1**, 223 (1957).
 - [42] M. Büttiker, Y. Imry, R. Landauer, and S. Pinhas, *Physical Review B* **31**, 6207 (1985).
 - [43] M. Biondi, S. Schmidt, G. Blatter, and H. E. Türeci, *Physical Review A* **89**, 025801 (2014).
 - [44] P. Longo, P. Schmitteckert, and K. Busch, *Physical Review Letters* **104**, 023602 (2010).
 - [45] A. Biella, arXiv:1407.6562 (2014).
 - [46] A. Biella, F. Borgonovi, R. Kaiser, and G. L. Celardo, *Europhysics Letters* **103**, 57009 (2013).
 - [47] G. Celardo, A. Biella, L. Kaplan, and F. Borgonovi, *Fortschritte der Physik* **61**, 250 (2013).
 - [48] V. M. Agranovich and Y. N. Gartstein, *Physical Review B* **75**, 075302 (2007).

- [49] J. Schachenmayer, B. P. Lanyon, C. F. Roos, and A. J. Daley, *Physical Review X* **3**, 031015 (2013).
 [50] Z.-X. Gong, M. Foss-Feig, S. Michalakakis, and A. V. Gorshkov, *Physical Review Letters* **113**, 030602 (2014).
 [51] M. Litinskaya, *Physical Review B* **77**, 155325 (2008).
 [52] J. Feist and F. J. Garcia-Vidal, arXiv:1409.2514 (2014).
 [53] F. Robicheaux, J. V. Hernández, T. Topçu, and L. D. Noordam, *Physical Review A* **70**, 042703 (2004).
 [54] A. Stute, B. Casabone, P. Schindler, T. Monz, P. O. Schmidt, B. Brandstätter, T. E. Northup, and R. Blatt, *Nature* **485**, 482 (2012).

SUPPLEMENTAL MATERIAL

Details on scattering calculation

It is convenient to write the reduced Hamiltonian for the cavity-coupled central N sites in its eigenbasis, $\sum_n \tilde{\Omega}_n \Pi_n^\dagger \Pi_n$, where the projectors $\Pi_n = |\text{vac}\rangle \langle n|$ destroy an excitation in the eigenstates $|n\rangle$. Since the total Hamiltonian $H = H_0 + H_{\text{cav}}$ commutes with the excitation operator, i.e. $\sum_{i=1}^N \sigma_i^\dagger \sigma_i^- + \sum_n \Pi_n^\dagger \Pi_n$, the one excitation ansatz can be written as

$$|\psi_q\rangle = \left[\sum_{i=1}^M C_{i,q}^{(l)} \sigma_i^\dagger + \sum_n p_q^n P_n^\dagger + \sum_{i=M+N+1}^N C_{i,q}^{(r)} \sigma_i^\dagger \right] |\text{vac}\rangle. \quad (3)$$

For the single exciton scattering $C_{i,q}^{(l)} \approx e^{-iq(i-M)} + r_q e^{iq(i-M)}$ and $C_{i,q}^{(r)} \approx t_q e^{iq(i-M-N-1)}$. The Schrödinger equation $H|\psi_q\rangle = \omega_q |\psi_q\rangle$ with $\omega_q = \omega - 2J \cos(q)$ entails $t_q = -2i\beta/(\Gamma_l \Gamma_r + |\beta|^2)$ with:

$$\Gamma_{l,r} = 1 + \frac{i}{2v_g} \sum_n \frac{|J'_{n,l,r}|^2}{\omega_q - \tilde{\Omega}_n} \quad \beta = \frac{1}{2v_g} \sum_n \frac{J'_{n,l} J'^*_{n,r}}{\omega_q - \tilde{\Omega}_n}. \quad (4)$$

Couplings $J'_{n,l} = -J' \langle n | \sigma_{M+1}^\dagger | \text{vac} \rangle$ and $J'_{n,r} = -J' \langle n | \sigma_{M+N}^\dagger | \text{vac} \rangle$ involve exciton amplitudes at the leftmost and rightmost cavity-coupled sites. The $N+1$ eigenvalues $\tilde{\Omega}_n$ are found by solving the reduced Schrödinger equation for the central N sites. They obey the non-linear equation

$$\frac{g^2}{N(\tilde{\Omega}_n - \omega_0)} \sum_{k=1}^N \frac{\left(\sum_{i=1}^N \alpha_k^i \right)^2}{\tilde{\Omega}_n - \omega_k} = 1, \quad (5)$$

with $\alpha_k^i = \sqrt{2/(N+1)} \sin(\pi/(N+1)kj)$ satisfying $\sum_{k=1}^N \alpha_k^i \alpha_k^{i'} = \sum_{k=1}^N \alpha_k^i \alpha_{i'}^k = \delta_{i,i'}$.

However, open boundary conditions (OBC) do not allow for an analytical expression of the transmission amplitude t_q ; it can be obtained by using periodic boundary conditions (PBC). Fourier transforms of the spin operators,

$$\sigma_k^\dagger = \frac{1}{\sqrt{N}} \sum_{j=M+1}^{M+N} \sigma_j^\dagger e^{i \frac{2\pi}{N} kj}, \quad (6)$$

allow to factorize the superradiant mode σ_0^\pm as well as to introduce the polaritons through the transformations $u^\dagger = (a^\dagger + \sigma_0^\dagger)/\sqrt{2}$ and $d^\dagger = (a^\dagger - \sigma_0^\dagger)/\sqrt{2}$. The Hamiltonian can then be diagonalized as $\tilde{\Omega}_u |u\rangle \langle u| + \tilde{\Omega}_d |d\rangle \langle d| + \sum_{k=1}^{N-1} \tilde{\Omega}_k \sigma_k^\dagger \sigma_k^-$ with polariton energies $\tilde{\Omega}_{u,d} = \omega_0 - J \pm g\sqrt{N}$. The energies of the $N-1$ uncoupled cavity modes are instead $\tilde{\Omega}_k = \omega_0 - 2J \cos(2\pi k/N)$. These also make the evaluation of coefficients β and $\Gamma_l = \Gamma_r = \Gamma$ straightforward:

$$\beta = \frac{|J'|^2}{2NJ \sin(q)} \left[\frac{1}{\omega_q - \tilde{\Omega}_u} + \frac{1}{\omega_q - \tilde{\Omega}_d} + \sum_{k=1}^{N-1} \frac{1}{\omega_q - \tilde{\Omega}_k} \right], \quad (7)$$

$$\Gamma = 1 + i\beta. \quad (8)$$

In fact $T_q = 1/(1 + \beta^{-2}/4)$. We also looked for transmission resonances in case of a site-dependent coupling g_i . In this case Eq. (5) reduces to

$$\frac{1}{N(\tilde{\Omega}_n - \omega_0)} \sum_{k=1}^N \frac{\left(\sum_{i=1}^N g_i \alpha_k^i \right)^2}{\tilde{\Omega}_n - \omega_k} = 1, \quad (9)$$

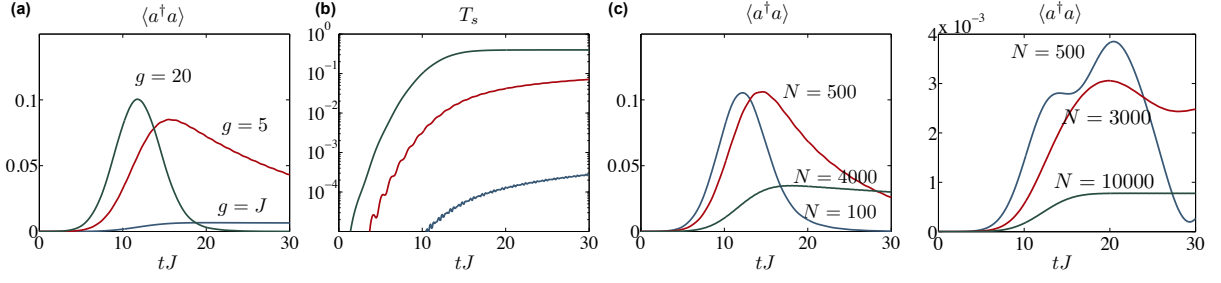


FIG. 4. *Time-evolution in different regimes* – (a) Evolution of the cavity occupation for the parameters of Fig. 2. $N = 1000$. The crossover from the $\sim g^4$ to the $\sim g$ regime happens for $g \gtrsim 10J$. This is exactly the value below which excitations remain in the cavity and the scattering theory breaks down. (b) The corresponding time-evolution of the transmission. Only for $g = 20$ the value saturates on the short time-scale. (c) The same crossover is visible when keeping $g = 5J$ fixed and increasing N , i.e. this crossover happens when the $\sim 1/\sqrt{N}$ scaling changes to a $\sim 1/N^2$ scaling. (d) In the case of disorder we always have the situation that excitations remain in the cavity. Interestingly for systems up to $N = 3000$ complex dynamics of the cavity occupation takes place. For larger N we have a similar situation as in the case without disorder and small g , i.e. part of the excitation is stuck in the cavity (and constant). Note also that in the disorder case the occupation is much smaller.

and the polariton peaks are at $\tilde{\Omega}_{u,d} = \omega_0 - J \pm \sqrt{\sum_{i=1}^N g_i}$.

Comparison analytics and numerics

We check under which circumstances our scattering theory gives agreement with the numerics. The condition that has to be met is that we have to be in the elastic scattering limit, i.e. the excitation goes fully in and out of the cavity on the time-scale of the experiment/simulation. Whether this is met can be checked by looking at the time evolution of the occupation number of the cavity mode. We analyze this in Fig. 4, where we show examples of the different regimes. In addition we check to what extent the height and peak-position of our transmission spectrum, which we calculate fully numerically, agrees with the analytical expectation. Results are shown in Fig. 5

Realistic semiconductor situation

The dipole moment for typical molecules is $d = e \times 0.75 \text{ nm}$. Given a spacing of $x = 3 \text{ nm}$ this yields a tunneling constant between nearest neighbors of $J = d^2 / (4\pi\epsilon_0 x^3) \approx 0.03 \text{ eV}$. According to [12] a Rabi-splitting of $\Omega_R \approx 1 \text{ eV} = 2g\sqrt{N}$ can be achieved for 10^5 molecules. Thus, a value of $g \approx 0.0016 \text{ eV} \approx 0.05J$ is realistic. Typical noise in the position is given by $\delta x = 0.2 \text{ nm}$, which is a fluctuation of 7% in x and yields a fluctuation of 20% in J . Finally, a typical level spacing is $\omega = 2 \text{ eV} \approx 70J$.

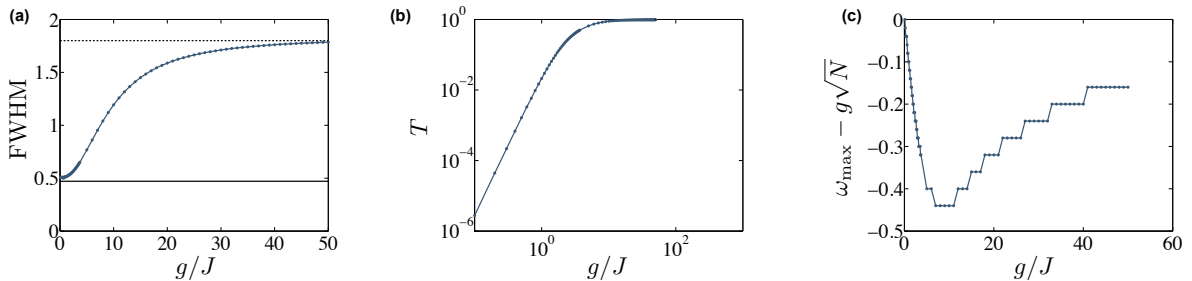


FIG. 5. *Numerical evaluation of the transmission peaks* (a) The FWHM as function of g for the numerical results from the scattering experiment ($N = 100$, $\delta_x = 20$, $\delta_0 = 5$, $J = 0$, $J' = 1.5\sqrt{2N}/\delta$). The lower solid line indicates the expected energy width of the wave packet. The upper dashed line is the expected transmission peak width from our analytical calculation (b) The corresponding transmission at the maximum peak position. The second kink from Fig. 2 disappears (and is thus related to the detuning) (c) the detuning from the analytical expected polariton peak-position.

Rydberg atoms – The XY model we consider in this manuscript can be realized in a *Rydberg lattice gas* [32]. Here with a first pulse a Rydberg $|nS\rangle$ state lattice is created by using the dipole blockade. Then these states are coupled to another $|n'P\rangle$ state that serves as second spin state. For example, in [32] the states $|60S_{1/2}\rangle$ and $|59P_{3/2}\rangle$ are used (^{87}Rb atoms). The level spacing is 18.5 GHz. A transition dipole moment between these states is Rydberg-typically ($d \sim n^2$) very large and on the order of $d = 2000 ea_0$. Resonant microwave cavities for transition frequencies of 51 GHz with dipole moments of $1000 ea_0$ and coupling strengths of $g \approx 300$ kHz (Q-factor of 3×10^8) have been successfully engineered [37]. Since $g \sim d\sqrt{\omega_0}$, couplings of $g \approx 350$ kHz are within reach. On the other hand, for a separation of $20 \mu\text{m}$, typical nearest neighbor tunneling is on order of 80 kHz [53] and thus g much larger than J is clearly possible. For a Q factor of 10^8 , the decay rate would be 1 kHz and thus negligible compared to g and J . The lifetime of the Rydberg states can be on the order of tens of milliseconds and therefore also spontaneous emissions can be safely neglected.

Polar molecules – The same type of microwave cavities could be used for systems of *polar molecules* in optical lattices, where rotational states (spacing typically ~ 2 GHz) can be used as spin-states. In these systems $J \approx 50$ Hz has been successfully observed in a recent experiment [33, 34]. While much stronger couplings $g \gg J$ can be engineered for these systems, a challenge might be to build a cavity with a sufficiently large Q-factor. For example, for $Q = 10^8$, $\kappa = 125$ Hz and thus larger than J . The lifetime of the states is sufficiently long to observe coherent dynamics over ~ 0.1 s [33].

Cold ions – In the domain of optical transitions, setups with *ions* in linear Paul traps might be considered. In these experiments tunneling rates of $J \approx 400$ Hz can be achieved [2]. Note that since in these experiments the hopping is mediated by motional degrees of freedom of the ion-crystal, also long-range hoppings are important. Typical decay exponents range from $\alpha = 0.1$ (almost all-to-all interactions) to $\alpha = 2$. In the all-to-all case no cavity is required at all. Nevertheless, ion in cavities with couplings of $g \sim 10$ MHz (with $\kappa \sim \text{MHz}$) [54] can be engineered. Thus, here also very strong coupling in the regime $\kappa \gg J$ could be achieved. We also numerically verified ultra-fast transmission in the case of an all-to-all coupling $H_\infty = J_\infty \sum_{i,j} \sigma_i^- \sigma_j^+$. In Fig. 6 we use the same wave-packet as in Fig. 2. Instead of coupling the sites $i = M + 1, \dots, M + N$ to a cavity however, we couple them collectively via H_∞ . Again we find ultra-fast transmission peaks with $T_{t_s} = 1$, however now they appear at values of $\Delta \sim \Omega_0 = NJ_\infty$, which corresponds to the eigenenergy of the dominant eigenvalue of the all-to-all Hamiltonian.

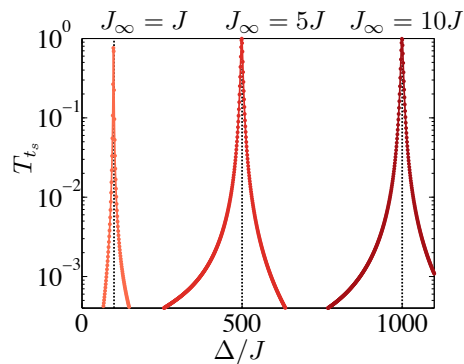


FIG. 6. *All-to-all interactions* – Wave-packet identical to the one in Fig. 2, $N = 100$. The N particles are coupled by H_∞ (no cavity). T_{t_s} as function of Δ shows peak at the values of the eigenenergy of the dominant eigenvalue of H_∞